Available online at www.sciencedirect.com
SCIENCE DIRECT
Journal of Magnetic Resonance 181 (2006) 280–286
JMR Journal of Magnetic Resonance
www.elsevier.com/locate/jmr

A Davies/Hahn multi-sequence for studies of spin relaxation in pulsed ENDOR

Tran-Chin Yang, Brian M. Hoffman *

Department of Chemistry, Northwestern University, Evanston, IL 60208-3003, USA

Received 18 January 2006; revised 12 May 2006
Available online 14 June 2006

Abstract

We extend earlier studies of the effects of relaxation on the intensities of pulsed ENDOR signals by introducing a Davies/Hahn (D/H) pulsed ENDOR multi-sequence that corresponds to a series of Davies sequences with the preparation pulse 'turned off'. In this pulse train, the Hahn [π/2, π] detection pulse pair of sequence $n-1$ both generates the echo detected for that sequence and acts as the preparation portion of sequence n, in effect replacing the π preparation pulse of the Davies sequence. We show both theoretically, through a master-equation approach, and with both $^{1}H(I = 1/2)$ and $^{14}N(I = 1)$ ENDOR experiments on the non-heme Fe enzymes, superoxide reductase (SOR) ($S = 1/2$) and AntDO ($S = 3/2$), that under conditions of high electron–spin polarization (high microwave frequency/low temperature) the D/H multi-sequence allows simplification of ENDOR spectra by suppression of nuclear transitions associated with the $m_S = +1/2$ (α) manifold. As such suppression depends on the sign of A, it allows determination of this sign. The suppression as a function of the time between individual sequences is found to exhibit behaviors that can be classified into three regimes of the ratio of cross-relaxation to spin–lattice relaxation rates: strong cross-relaxation (X-case); comparable rates (XL); negligible cross relaxation (L). Interestingly, the ENDOR behavior of the $S = 1/2$ SOR center indicates it is an L case, while the $S = 3/2$ AntDO is an XL case. Overall, the D/H protocol appears to be a robust and general tool for using relaxation effects to manipulate ENDOR spectra.

Keywords: Pulsed ENDOR; Spin–lattice relaxation; Hyperfine coupling sign

1. Introduction

The most widely used pulsed-ENDOR sequences were devised by Mims [1], and Davies [2], although modified pulse sequences have been described [3–5]. These two sequences are well known to allow simplification of ENDOR spectra through suppression of signals where the *magnitude* of the hyperfine coupling (A) falls in a selected range. Thus, changing the pulse lengths in a Davies-type ENDOR experiment yields suppression effects known as self-ELDOR (electron–electron double resonance) or POSHE (proton suppression, heteronuclear enhancement) [4,6]. Variation in the interval between the 1st and 2nd microwave pulse of a Mims sequence offers a more delicate means of suppression based on the magnitude of A. It is also possible to simplify ENDOR spectra in ways that depend on the *sign* of A. An ENDOR spectrum from a hyperfine-coupled nucleus consists of branches at frequencies, $\nu_{\pm} = |A/2 \pm \nu_N|$. One of these is associated with the $m_S = +1/2$ (α) electron spin projection and the other with $m_S = -1/2$ (β); which value of m_S is associated with ν_+/ν_- is determined by the sign of A. Complete suppression of one of the two branches can be achieved through use of circularly polarized radio frequency (RF) fields [7]. The effects of electron/nuclear relaxation also can cause unequal intensities of the ν_+/ν_- branches, and it has long been clear that this is related to relaxation effects that are linked to the sign of A [8–10].

The systematic treatment of these effects was initiated by Bennebroek et al., who observed an "anomalous"

* Corresponding author. Fax: +1 847 491 7713.
E-mail address: bmh@northwestern.edu (B.M. Hoffman).

1090-7807/$ - see front matter © 2006 Elsevier Inc. All rights reserved.
doi:10.1016/j.jmr.2006.05.011

positive sign in Mims ENDOR experiments carried out under conditions of high electron–spin polarization. This was interpreted as an effect of spin–lattice relaxation [11]. A thorough analysis of such effects in Davies-type experiments was presented by Epel et al. [12]. They showed that the absolute signs of the electron–nuclear hyperfine coupling constant can be determined by varying the mixing time (t_{mix}) and/or repetition time (t_R) in a Davies pulsed ENDOR multi-sequence (Scheme 1). Their analysis explains the effects previously observed in pulsed ENDOR, and the approach is a very attractive addition to earlier pulse 'TRIPLE' ENDOR techniques for sign determination. Those either utilize a second microwave or RF source [4,13], or rely on heteronuclear modulation effects [14]. The present work grows out of an unsuccessful attempt to use the Davies multi-sequence to determine the signs of hyperfine couplings in the $S = 3/2$ nitrosyl-ferrous [NO-Fe^{II}] center of the non-heme Fe enzyme anthranilate dioxygenase, AntDO [15,16]. These attempts have led us to extend the work of Epel et al. by introducing a Davies/Hahn (D/H) pulsed ENDOR multi-sequence, Scheme 1, that also allows simplification of ENDOR spectra by suppression effects that depend on the sign of A, and thereby allows determination of this sign. We follow the approach of Epel et al. in presenting a general master-equation model for the ENDOR intensities of this multi-sequence as applied to the four-level system of a nuclear spin $I = 1/2$ coupled to an electron spin $S = 1/2$; the treatment includes the effects of spin–lattice and cross relaxation and electron–spin polarization. The model indicates that the relative intensities of the ν_+/ν_- branches in the D/H multi-sequence vary with t_R in a fashion that depends on the sign of A. The practical utility of the scheme is illustrated by application to the ^{1}H ENDOR signals from the non-heme-Fe(III) enzymes, superoxide-reductase (SOR) [17] and [NO-Fe^{II}]-AntDO. Further, the D/H multi-sequence is shown to be effective in controlling the intensities of the ν_+/ν_- branches of $^{14}N(I = 1)$ signals from [NO-Fe^{II}]-AntDO, and thereby yields the signs of the ^{14}N couplings, as well. Thus, this protocol appears to be a robust and general tool for using relaxation effects to manipulate ENDOR spectra.

2. Theory

In the Davies ENDOR pulse multi-sequence [12], Scheme 1, a preparation π pulse is repeated in each sequence with a delay interval of t_R, and drives the system to a non-thermal-equilibrium steady state after multiple repetitions of the individual cycles. The D/H multi-sequence is programmed as multiple Davies sequences separated by delay time, t_R, but with the preparation π pulse 'turned off'. In this pulse train, the Hahn detection pulse pair of sequence $n-1$ not only generates the echo detected for that sequence, but also acts as the preparation portion of sequence n, in effect replacing the π preparation pulse of the Davies sequence. The pair is equivalent to a single π/2 pulse, rather than the Davies π pulse, if relaxation between the two Hahn pulses is ignored. Thus it is the Hahn pairs of a D/H multi-sequence that act to drive the system to a non-thermal-equilibrium steady state.

We wish to determine the t_R dependence of the D/H multi-sequence applied to a system with electron spin $S = 1/2$ and nuclear spin $I = 1/2$. The energy levels of this system in the high-field limit can be described by Fig. 1: the electronic Zeeman interaction splits the $m_S = \pm 1/2$ manifolds, which are further split into $|m_S, m_I\rangle$ states by the smaller hyperfine interaction and nuclear Zeeman terms. The populations of the four $|m_S, m_I\rangle$ states at any time (t) are written in vector form, $\mathbf{n}(t) = (n_1(t), n_2(t), n_3(t), n_4(t))^T$ (where T is the transpose of the column vector). The electronic relaxation rates W_{ij} (= W_{12}, W_{21}, W_{34}, or W_{43}), cross relaxation rates W_{xij} (= W_{x14}, W_{x41}, W_{x23}, or W_{x32}), and nuclear relaxation rates W_{nij} (= W_{n13}, W_{n31},

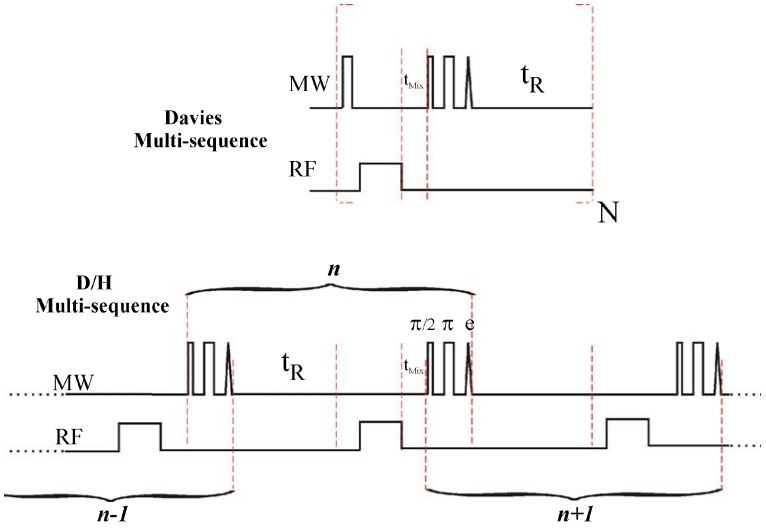

Scheme 1.

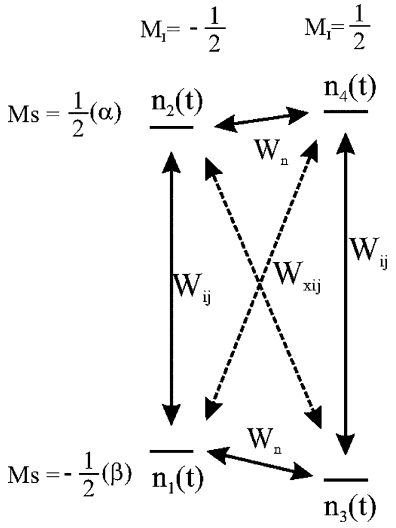

Fig. 1. Energy level diagram at high magnetic field for the system with $S = 1/2$ and $I = 1/2$ where $n_i(t)$ indicates the total spins at time t in state i. And the electronic, nuclear, and crossing relaxation rates between i and j states are symbolized as W_{ij}, W_n, and W_{xij}, respectively.

W_{n24}, or W_{n42}) describe the dissipative transitions between states i and j.

Thermal equilibrium, characterized by Boltzmann populations, $\mathbf{n}_0 = (n_{10}, n_{20}, n_{30}, n_{40})^{\mathrm{T}}$, is achieved by a balance of relaxation rates as defined in Fig. 1. At the microwave frequencies used in EPR, even at low temperature, the nuclear splittings are much smaller than thermal energies. Thus, the thermal-equilibrium populations may be described as

$$n_{10} = n_{30}, \quad n_{20} = n_{40}$$

Thermal equilibrium implies the following relation between populations, relaxation rates, and temperature

$$\frac{n_{20}}{n_{10}} = \frac{W_{12}}{W_{21}} = \frac{W_{x14}}{W_{x41}} = \mathrm{e}^{(-\mathrm{h}\nu/\mathrm{kT})} \tag{1}$$

where $\mathrm{h}\nu$ is the Zeeman energy splitting between $\mathrm{m}_S = \pm 1/2$ states, and k is the Boltzmann constant. We further assume that the relaxation rates obey the relations,

$$W_{12} = W_{34}, W_{21} = W_{43}, W_{x32} = W_{x14}, W_{x23} = W_{x41},$$
$$W_{n13} = W_{n31} = W_{n24} = W_{n42} = W_n,$$
$$T_{1\mathrm{e}} = (W_{12} + W_{21})^{-1} = (W_{34} + W_{43})^{-1}$$

In the absence of time-varying fields, the populations vary with time according to the master equation [18],

$$\mathrm{d}\mathbf{n}(\mathbf{t})/\mathrm{d}t = -\Gamma\,\mathbf{n}(\mathbf{t}), \quad \text{or} \quad \mathbf{n}(\mathbf{t}) = \mathrm{e}^{-\Gamma t}\,\mathbf{n}(\mathbf{t}=\mathbf{0}) \tag{2}$$

where Γ is the relaxation matrix,

$$\Gamma = \begin{bmatrix} W_{12} + W_n + W_{x14} & -W_{21} & -W_n & -W_{x41} \\ -W_{12} & W_{21} + W_{x23} + W_n & -W_{x32} & -W_n \\ -W_n & -W_{x23} & W_n + W_{x32} + W_{34} & -W_{43} \\ -W_{x14} & -W_n & -W_{34} & W_{x41} + W_n + W_{43} \end{bmatrix}$$

and $\mathbf{n}(\mathbf{t} = \mathbf{0})$ is the initial population vector. In the application of the multi-Davies sequence to control asymmetry of the ν_+/ν_- branches, Epel et al. consider varying both the mixing and repetition times, t_{mix}, t_{R}. In the D/H sequence, we focus on the repetition time t_{R} as the interval to be examined. As t_{R} is on the order of milliseconds while $[T + t_{\mathrm{mix}}]$ typically is $\sim$60 μs, we set $[T + t_{\mathrm{mix}}] = 0$ in our calculations.

Following the development of Epel et al., to model the D/H experiment we assume a selective microwave pulse excites the $m_S = -1/2 \leftrightarrow 1/2$ transition associated with the nuclear spin quantum number $m_I = -1/2$; the results are the same for if we treat the $m_I = +1/2$ transition. The propagator P_{D} of a two-pulse Hahn echo $[\pi/2 - \pi]$ detection pulse sequence applied to the $m_I = -1/2$ transition of a system with spin populations $\mathbf{n}(\mathbf{t})$ can be expressed by the matrix,

$$P_{\mathrm{D}} = \begin{bmatrix} \frac{1}{2} & \frac{1}{2} & 0 & 0 \\ \frac{1}{2} & \frac{1}{2} & 0 & 0 \\ 0 & 0 & 1 & 0 \\ 0 & 0 & 0 & 1 \end{bmatrix}$$

if relaxation between the two pulses is ignored. We further assume an inverting (π) RF pulse, in which case the RF propagators for NMR transitions in the $m_S = 1/2$ (α) and $-1/2$ (β) electron manifolds are, respectively,

$$P^{\alpha}_{\mathrm{rf}} = \begin{bmatrix} 1 & 0 & 0 & 0 \\ 0 & 0 & 0 & 1 \\ 0 & 0 & 1 & 0 \\ 0 & 1 & 0 & 0 \end{bmatrix} \quad \text{and} \quad P^{\beta}_{\mathrm{rf}} = \begin{bmatrix} 0 & 0 & 1 & 0 \\ 0 & 1 & 0 & 0 \\ 1 & 0 & 0 & 0 \\ 0 & 0 & 0 & 1 \end{bmatrix}$$

The steady-state populations in the nth of a series of D/H sequences, just before applying the Hahn detection pulses, can be described by steady-state equations,

$$\mathrm{e}^{-\Gamma t_{\mathrm{R}}}\; P_{\mathrm{D}}\; \mathbf{n}(\mathbf{t_R}) = \mathbf{n}(\mathbf{t_R}) \tag{3a}$$

$$P^{\alpha}_{\mathrm{rf}}\; \mathrm{e}^{-\Gamma t_{\mathrm{R}}}\; P_{\mathrm{D}}\; \mathbf{n}(\mathbf{t_R}) = \mathbf{n}(\mathbf{t_R}) \tag{3b}$$

$$P^{\beta}_{\mathrm{rf}}\; \mathrm{e}^{-\Gamma t_{\mathrm{R}}}\; P_{\mathrm{D}}\; \mathbf{n}(\mathbf{t_R}) = \mathbf{n}(\mathbf{t_R}) \tag{3c}$$

These correspond to measurements with "rf off" (Eq. (3a)), "rf on" for nuclear transitions in the $m_S = +1/2$ (α) (Eq. (3b)), and for $m_S = -1/2$ (β) (Eq. (3c)) nuclear transitions, respectively. The echo intensity is given by

$$I_{\mathrm{echo}}(t_{\mathrm{R}}) = n_1(t_{\mathrm{R}}) - n_2(t_{\mathrm{R}}) \tag{4}$$

and the ENDOR effect (EE) [19] is equal to the difference of the echo intensity between "rf on" and "rf off"; for

example, for a nuclear transition in the $m_S = +1/2$ manifold,

$$\mathrm{EE}^{\alpha}(t_R) = I_{\mathrm{echo}}^{\mathrm{on},\alpha}(t_R) - I_{\mathrm{echo}}^{\mathrm{off}}(t_R) \quad (5)$$

3. Calculation

Eqs. (1–5) were used to calculate the ENDOR effect EE as a function of the repetition time t_R, for the D/H multi-sequence over a range of relaxation parameters; the calculations were performed to model our experiments at $T = 2$ K with $\nu = 35$ GHz, corresponding to the ratio $\beta_B = h\nu/kT = 0.84$. This ratio in fact is the same as that used by Epel et al. in describing their W-band experiments (95 GHz) at 5.5 K. Stated differently, the electron–spin polarization in W-band experiments at 5.5 K is the same as in Q-band experiments at 2 K. As the echo is measured in every sequence, for the average echo intensity to reflect the true steady state described by these equations, the steady state of Eq. (3) should be reached within a small number of sequences relative to the total number. In fact, the simulation converges very quickly; after just three cycles, the spin populations generally reach ~96% of their steady state values. Therefore, a multi-sequence in which we collect $N = 50$ or more echoes for each ENDOR frequency in each frequency scan will provide reliable results.

In the calculation, four parameters must be input, $\beta_B = 0.84$ here, T_{1e}, W_n, and W_x ($= W_{x23} + W_{x32} = W_{x14} + W_{x41}$). For a metalloprotein at 2 K, the nuclear relaxation rate normally is much slower than that of electrons. Therefore, we ignore the nuclear term, $W_n = 0$, and examine three different cases: (i) strong cross-relaxation (X-case), $W_x \gg W_e$ ($= T_{1e}^{-1}$); (ii) comparable cross and spin–lattice relaxation (XL-case), $W_x \approx W_e$; (iii) weak cross-relaxation (L), $W_x \ll W_e$. We set $T_{1e} = 7$ ms, an approximate value measured from an inversion recovery experiment. The ENDOR effects vs. repetition time calculated for the three cases are shown in Fig. 2 with total spin populations normalized to 1.

The calculations show that two features always hold: (1) the phase of the $m_S = -1/2$ ENDOR transition is positive while that from the $m_S = 1/2$ state can be either positive, zero, or negative depending on the relaxation rates W_x and W_e, and t_R, etc., where the phase is defined relative to the positive-phase two-pulse Hahn echo described in Eq. (5). (2) $\mathrm{EE}^{\beta} > \mathrm{EE}^{\alpha}$ (algebraically) for any t_R. As a result of these findings, if the D/H sequence causes a substantial asymmetry in the intensities of the ν_+/ν_- branches, the sign of A can be read off without comparison to calculations. Interestingly, in the Davies multi-sequence, both branches of the spectrum can have either positive or negative phase, depending on the relaxation parameters. Although this analysis of the D/H scheme, as is that of Epel et al. for the Davies scheme, is formulated for a nucleus with $I = 1/2$, it is to be expected that the predictions will be semi-quantitatively applicable to $^{14}\mathrm{N}(I = 1)$; we show below that this is the case.

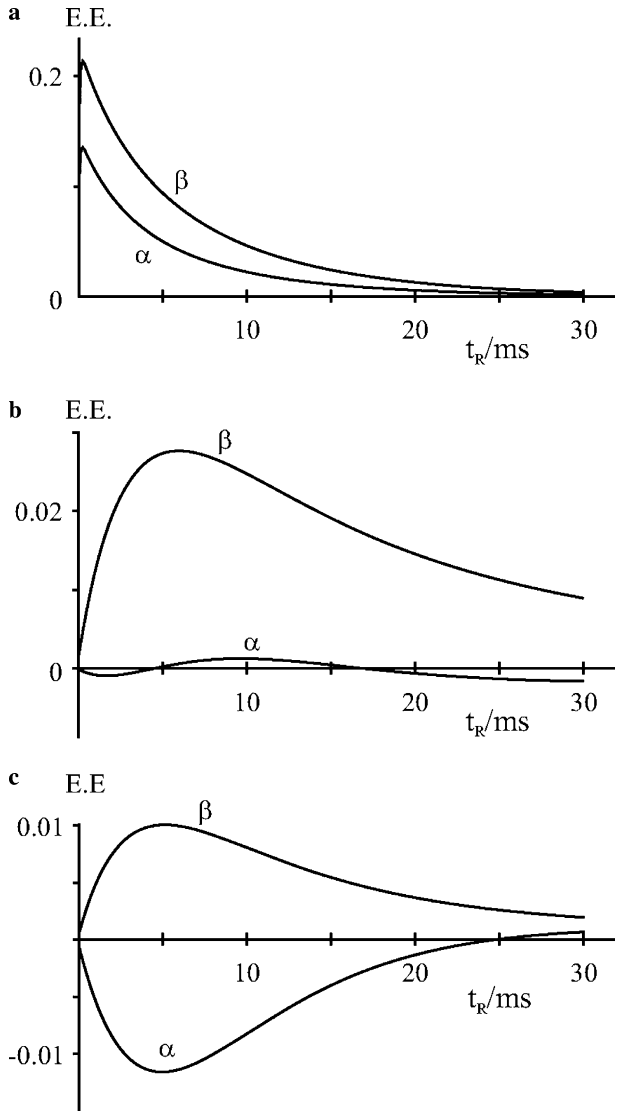

Fig. 2. The intensities of ENDOR Effect (EE) vs. the repetition time t_R were calculated from Eq. (1–5) with $T_{1e} = W_e^{-1} = 7$ ms, $W_n = 10^{-10}$ ms^{-1}. Other relaxation parameters are: (a) X-case. $W_x = 100\ W_e$; (b) XL-case. $W_x = 0.3\ W_e$; (c) L-case. $W_x = 10^{-9}\ W_e$. The microwave frequency and temperature were set at 35 GHz and 2 K, respectively.

4. Experimental results and discussion

Fe(III)-CN SOR has a ferric non-heme Fe(III) center with four histidyl nitrogen ligands forming a plane, a cysteinyl thiolate as one axial ligand, and CN^- as the other. Fig. 3 shows 35 GHz ^{1}H ENDOR spectra collected at $g = 1.94$ ($\sim g_3$); the indicated ν_+/ν_- doublets for the two cysteinyl β protons have $A(H1,2) \approx 15, 8$ MHz. The Davies spectrum taken with $t_R = 10$ ms, which has excellent S/N, has the intensity of the ν_- peak of H1 clearly greater than that of ν_+. This ratio does not change appreciably with a decrease to $t_R = 2$ ms, while S/N clearly is appreciably reduced; increases in t_R increase the S/N slightly, without additional change in the ν_+/ν_- intensity ratio. Thus, the sign of A is not accessible with this sequence. However, in the spectrum taken with the D/H multi-sequence at

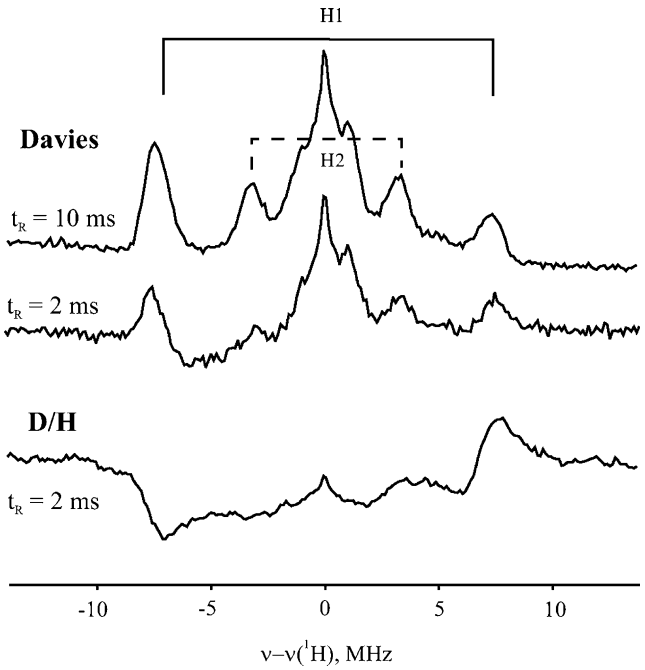

Fig. 3. Q-band pulsed ^{1}H ENDOR spectra for SOR-CN. The top two spectra were collected with the Davies sequence ($t_R = 2$, 10 ms), the bottom one with the D/H multi-sequence ($t_R = 2$ ms). *Conditions*: mw = 34.685 GHz, $\pi/2 = 40$ ns; RF = 100 μs with 100 kHz bandwidth broadened; resolution = 256 points; data average = 2000 transients/point; $T = 2$ K.

$t_R = 2$ ms, the ν_+ peak of H1 retains its positive sense while the ν_- peak has inverted. According to the above calculation, this identifies ν_+ with the $m_S = -1/2$ (β) transition, and thus fixes the sign of the hyperfine coupling: A(H1) = +15 MHz. Although we did not experimentally examine the entire accessible range, 2 ms $< t_R <$ 20 ms for the D/H multi-sequence applied to the ^{1}H ENDOR signals from SOR-CN, the observation that the ν_+ and ν_- peaks have opposite phase but similar intensities in the D/H experiment suggests that cross-relaxation in this $S = 1/2$ center is negligible, and that the Fe(III) $S = 1/2$ center is described by the case (L) of Fig. 2c.

The present work began with the study of AntDO. Binding the O_2-surrogate, NO, to a non-heme Fe(II) enzyme such as AntDO produces an $S = 3/2$ center that is quite amenable to ENDOR study [20,21]. The coordination sphere of the Fe of NO-AntDO is thought to include the NO, one solvent (OH_x), the nitrogens of two histidyl imidazoles, and the oxygen(s) of an aspartate carboxylate [15,16]. Fig. 4 (top) shows the complete conventional 35 GHz Davies pulsed ENDOR spectrum of this enzyme collected at 2 K; the field corresponds to g = 4.13 (close to g_1) where the proton Larmor frequency is $\nu_H \sim 25$ MHz. The spectrum shows numerous ^{1}H doublets centered at ν_H and split by hyperfine couplings as large as $A \sim 20$ MHz. To lower frequencies, $\nu \lesssim 17$ MHz, are two clusters of resonance from the coordinated ^{14}N; it is not possible to know whether additional ^{14}N features are obscured by the proton resonances. The figure includes a putative

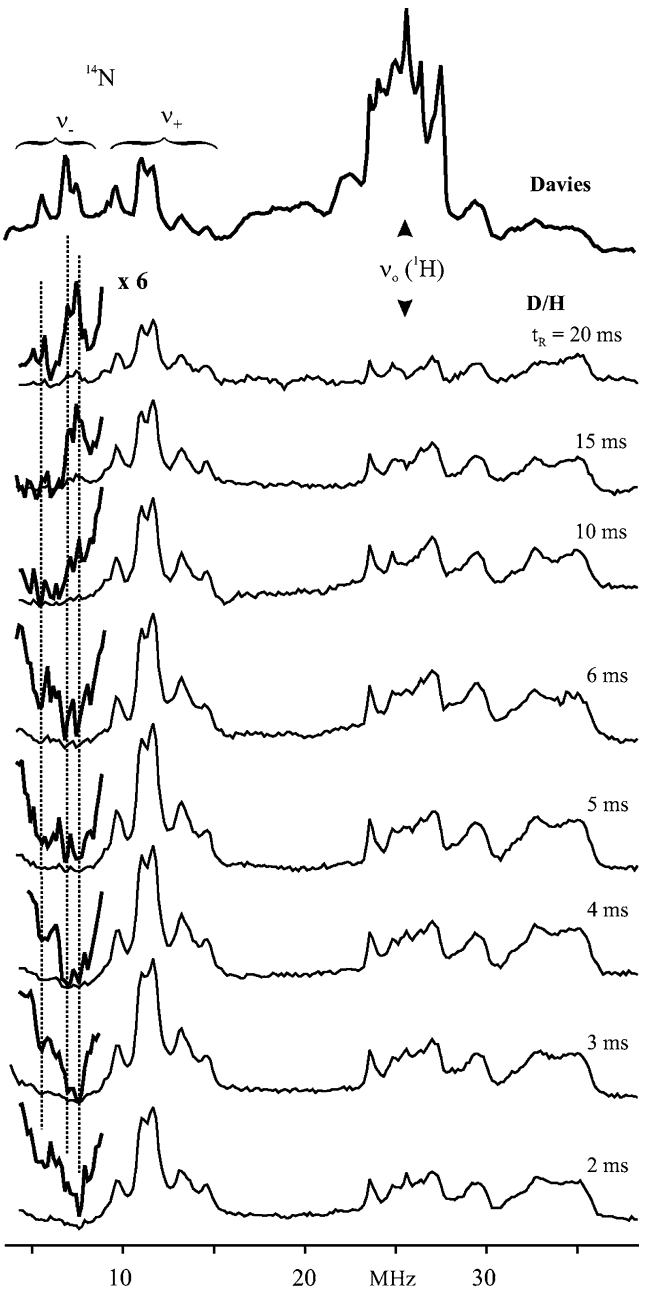

Fig. 4. Q-band ENDOR spectra for natural abundance AntDO were collected with the standard Davies sequence (t_R = 10 ms) (top) and for the D/H multi-sequence as a function of repetition time, t_R (all other). *Conditions*: mw = 34.807 GHz, $\pi/2 = 40$ ns; RF pulse (T) = t_{mix} = 10 μs, resolution = 256 points; data average = 500 transients/point; $T = 2$ K.

assignment of the two sets of ^{14}N signals as the ν_+ and ν_- branches of the spectrum from one or more ^{14}N in which the pattern is centered at $A(^{14}N)/2$ and split by $2\nu_N$, each branch with a further quadrupole splitting, 3P: $\nu_\pm(\pm) = |A/2 \pm \nu_N \pm 3P/2|$. However, it is also possible that the low frequency branches (ν_-) of spectra from bound nitrogen(s) are suppressed by relaxation effects in these spectra collected at 2 K and 35 GHz [8,9]. If this is happening here, the ^{14}N features assigned as 'ν_+' and 'ν_-' branches might alternatively be the ν_+ branches of non-equivalent

histidines, neither of which shows a ν_- branch with significant intensity.

We attempted to resolve these questions through use of the multi-Davies sequence of Scheme 1 to vary the asymmetry between the intensities of ^{1}H and ^{14}N ν_+ and ν_- branches. However, in experiments performed with values for $2 \leqslant t_R \leqslant 20$ ms, we could neither generate substantial asymmetry of the ^{1}H signals nor modify the ^{14}N spectra (Fig 1S); this is illustrated in a sample Davies ENDOR spectrum of AntDO with $t_R = 10$ ms given at the top of Fig. 4. This difficulty led us to vary the length of the preparation pulse within the Davies sequence, as well as [t_R, t_{mix}]. In this exploration we arrived at the D/H multi-sequence which is able to generate asymmetries not only for the $I = 1/2$ proton signals of AntDO, but also to controllably generate asymmetries for the $I = 1$ ^{14}N signals, and thereby to resolve the questions posed about the AntDO Davies spectrum.

Application of the multi-D/H sequence to AntDO for repetition times, $2 < t_R < 20$ ms gave spectra shown in Fig. 4. Over the entire range of t_R, this sequence suppresses the ν_- branch of the ^{1}H signals with $A \gtrsim 5$ MHz. According to the analysis above, this shows that ν_+ for these protons must correspond to the $m_S = -1/2$ (β) branch, and therefore $A(H) > 0$ for all the strongly coupled protons.

Unsurprisingly, the D/H multi-sequence also modulates the relative intensities of the ^{14}N features assigned as the ν_+/ν_- branches. In addition, and presumably because of quadrupolar relaxation effects for the $I = 1$ nucleus that do not occur for the $I = 1/2$ proton, it also is possible to control the ν_+/ν_- intensity ratio with the D/H sequence through variation of t_R. The branch assigned as ν_+ retains its positive phase over the entire range of t_R, decreasing in intensity somewhat as t_R is lengthened from 2 to 20 ms. However, the ν_- branch has a negative phase at 2 ms. These resonances slowly increase (algebraically) in intensity as t_R increases; depending upon which feature is considered, it crosses zero somewhere about 10 ms. However, the intensity of this branch always is less than that of the ν_+ branch. First, this behavior confirms the assignment of the two groups of features as ν_+/ν_- branches, rather than as ν_+ branches from distinct types of ^{14}N. Second, as with the strongly coupled protons, this behavior shows that $\nu_+(^{14}N)$ must correspond to nuclear transitions associated with the $m_S = -1/2$ (β) state, and thus demonstrates that $A(^{14}N) > 0$. In work to be published elsewhere we have been able to assign the ^{14}N peaks to ^{14}N-histidine and to ^{14}NO. This involved the use of ^{15}N labelling, and relied not only on the manipulation of the nitrogen intensities, but on suppression of the ν_- branch of the 1H ENDOR spectrum, which allowed us to resolve ^{15}N peaks which would have otherwise masked by the proton ν_- branch.

The calculational scheme presented above for $I = 1/2$ can be used heuristically to discuss the ^{14}N results, and thereby to assess the relaxation parameters of AntDO, provided we recognize that the values used must be incorporating the influence of the nuclear relaxation, and keep in mind that the simulations also do not incorporate relaxation mechanisms such as spectral and spin diffusion. Indeed, the measurement of T_{1e} from an inversion recovery experiment likely suffers from the same difficulty. The plot of calculated ENDOR effects with comparable values for spin–lattice and cross-relaxation rates, case (XL) Fig. 2b, seems to best reflect the variation with t_R of the D/H multi-sequence ^{14}N signals that is presented in Fig. 4. Thus, unsurprisingly, the relaxation behaviors of the [NO-Fe(II)] ($S = 3/2$) (strong cross-relaxation) center of AntDO and the Fe(III) ($S = 1/2$) of SOR-CN (negligible cross-relaxation) are quite different.

We can learn more about the relaxation by asking, why doesn't the Davies multi-sequence work for the ^{14}N of AntDO? We have used the equations of Epel et al. to explore this question by simulating the Davies experiment. If we consider the case with comparable spin–lattice and cross-relaxation rates and use the same parameters used to create Fig. 2b, the simulated result, Fig. S2a, shows a slight negative phase for $m_S = -1/2$ (α) transitions at short t_R, contrary to experiment. However, if we use $T_{1e} = 1$ ms, rather than the nominal measured value of 7 ms, Fig. S2b–c, we achieve a reasonable fit to both the D/H and Davies experimental results, with negative phase for the α transitions in the D/H sequence but not for the Davies sequences. Therefore, the simulation parameters allow semi-quantitative understanding (correct order of the electronic relaxation rates), and the simulations do reflect the complementary nature of the two multi-sequences.

5. Summary

The D/H multi-sequence of Scheme 1 is found to be a robust and general way of modulating the intensities of the ν_+/ν_- branches of a pulsed ENDOR spectrum from an electron spin-polarized system in a way that allows a determination of the sign of the hyperfine coupling of a coupled nucleus. The master-equation description of this sequence was carried out for an electron spin $S = 1/2$ coupled to a nuclear spin of $I = 1/2$, and verification has been obtained from ^{1}H ENDOR spectra of the non-heme Fe center, SOR-CN. In addition the D/H sequence has been successfully applied to the ^{1}H and ^{14}N ENDOR spectra of the $S = 3/2$ [NO-Fe(II)] center of AntDO. The suppression as a function of t_R is found to exhibit behaviors that can be classified into three regimes of the ratio of cross-relaxation to spin–lattice relaxation rates: strong cross-relaxation (X-case); comparable rates (XL); negligible cross relaxation (L). Interestingly, the ENDOR behavior of the $S = 1/2$ SOR center indicates it is an L case, while the $S = 3/2$ AntDO is an XL case.

Acknowledgments

This work was supported by the NIH (HL13531). We thank Profs. Donald Kurtz and Michael Johnson for the enzyme samples.

Appendix A. Supplementary data

Supplementary data associated with this article can be found, in the online version, at doi:10.1016/j.jmr.2006.05.011.

References

[1] W.B. Mims, Pulsed endor experiments, Proc. Roy. Soc. Lond. 283 (1965) 452.
[2] E.R. Davies, A new pulse endor technique, Phys. Lett. A 47 (1974) 1.
[3] C. Gemperle, O.W. Sorensen, A. Schweiger, R.R. Ernst, Optimized polarization transfer in pulse endor experiments, J. Magn. Res. 87 (1990) 502.
[4] C. Gemperle, A. Schweiger, Pulsed electron-nuclear double resonance methodology, Chem. Rev. 91 (1991) 1481.
[5] A. Schweiger, G. Jeschke, Principles of Pulse Electron Paramagnetic Resonance, Oxford University Press, Oxford, UK, 2001, p. 578.
[6] P.E. Doan, C. Fan, C.E. Davoust, B.M. Hoffman, A simple method for hyperfine selective heteronuclear pulsed endor via proton suppression, J. Magn. Res. 95 (1991) 196.
[7] A. Schweiger, H.H. Guenthard, Electron nuclear double resonance with circularly polarized radio-frequency fields (cp-endor). Theory and applications, Mol. Phys. 42 (1981) 283.
[8] V.J. DeRose, K.E. Liu, S.J. Lippard, B.M. Hoffman, Investigation of the dinuclear fe center of methane monooxygenase by advanced paramagnetic resonance techniques: On the geometry of the dmso binding, J. Am. Chem. Soc. 118 (1996) 121.
[9] D. Burdi, J. Willems, P. Riggs-Gelasco, W. Antholine, J. Stubbe, B. Hoffman, The core structure of x generated in the assembly of the diiron cluster of ribonucleotide reductase: $^{17}o_2$ and h2^{17}o endor, J. Am. Chem. Soc. 120 (1998) 12910.
[10] R. Davydov, V. Kofman, J. Nocek, R.W. Noble, H. Hui, B.M. Hoffman, Conformational substrates of the oxyheme centers in α and β subunits of hemoglobin as disclosed by epr and endor studies of cryoreduced protein, Biochemistry 43 (2004) 6330.
[11] M.T. Bennebroek, J. Schmidt, Pulsed endor spectroscopy at large thermal spin polarizations and the absolute sign of the hyperfine interaction, J. Magn. Reson. 128 (1997) 199.
[12] B. Epel, A. Poppl, P. Manikandan, S. Vega, D. Goldfarb, The effect of spin relaxation on endor spectra recorded at high magnetic fields and low temperatures, J. Magn. Reson. 148 (2001) 388.
[13] H. Thomann, M. Bernardo, Pulsed electron-nuclear-electron triple resonance spectroscopy, Chem. Phys. Lett. 169 (1990) 5.
[14] P.E. Doan, M.J. Nelson, H. Jin, B.M. Hoffman, An implicit triple effect in mims pulsed endor: a sensitive new technique for determining signs of hyperfine couplings, J. Am. Chem. Soc. 118 (1996) 7014.
[15] D.M. Eby, Z.M. Beharry, E.D. Coulter, D.M. Kurtz Jr., E.L. Neidle, Characterization and evolution of anthranilate 1,2-dioxygenase from acinetobacter sp. Strain adp1, J. Bacteriol. 183 (2001) 109.
[16] Z.M. Beharry, D.M. Eby, E.D. Coulter, R. Viswanathan, E.L. Neidle, R.S. Phillips, D.M. Kurtz Jr., Histidine ligand protonation and redox potential in the rieske dioxygenases: role of a conserved aspartate in anthranilate 1,2-dioxygenase, Biochemistry 42 (2003) 13625.
[17] A.P. Yeh, Y. Hu, F.E. Jenney Jr., M.W. Adams, D.C. Rees, Structures of the superoxide reductase from *Pyrococcus furiosus* in the oxidized and reduced states, Biochemistry 39 (2000) 2499.
[18] C.P. Slichter, Principles of magnetic resonance, in: P. Fulde (Ed.), Springer Series in Solid-State Sciences, third ed., Springer-Verlag, Berlin, 1990, p. xi,655.
[19] Epel et al. use an alternative definition of ENDOR efficiency, EE/I_{echo}^{off}.
[20] T.-C. Yang, M.D. Wolfe, M.B. Neibergall, Y. Mekmouche, J.D. Lipscomb, B.M. Hoffman, Substrate binding to no-ferro-naphthalene 1,2-dioxygenase studied by high-resolution Q-band pulsed ^{2}H-endor spectroscopy, J. Am. Chem. Soc. 125 (2003) 7056.
[21] D.L. Tierney, A.M. Rocklin, J.D. Lipscomb, L. Que Jr., B.M. Hoffman, Endor studies of the ligation and structure of the non-heme iron site in acc oxidase, J. Am. Chem. Soc. 127 (2005) 7005.